Acta Odontologica Scandinavica, 2013; 71: 906–916

informa
healthcare

ORIGINAL ARTICLE

Periodontal ligament cell behavior on different titanium surfaces

SEMA S. HAKKI[1], PETEK KORKUSUZ[2], NUHAN PURALI[3], FEZA KORKUSUZ[4], BUKET S. BOZKURT[5], ERDOGAN E. HAKKI[6], M. ERCUMENT ONDER[4], ILKER GORUR[7], RAHIME M. NOHUTCU[8], MUHARREM TIMUCIN[9] & ADNAN OZTURK[7]

[1]*Department of Periodontology, Faculty of Dentistry, Selcuk University, Konya, Turkey,* [2]*Department of Histology and Embryology,* [3]*Department of Biophysics, Hacettepe University Faculty of Medicine, Ankara, Turkey,* [4]*Department of Biomedical Engineering and Medical Center, Middle East Technical University, Ankara, Turkey,* [5]*Research Center of Faculty of Dentistry,* [6]*Department of Soil Science and Plant Nutrition, Molecular Genetics & Biotechnology Laboratories, Faculty of Agriculture, Selcuk University, Konya, Turkey,* [7]*Department of Oral and Maxillofacial Surgery, Faculty of Dentistry, Ankara University, Ankara, Turkey,* [8]*Department of Periodontology, Faculty of Dentistry, Hacettepe University, Ankara, Turkey, and* [9]*Department of Metallurgical and Materials Engineering, Faculty of Engineering, Middle East Technical University, Ankara, Turkey*

Abstract

Aim. The purpose of this study was to investigate proliferation, morphology, mineralization and mRNA expressions of mineralized tissue associated proteins of PDL cells on smooth (S), sandblasted small-grit (SSG), sandblasted large-grit (SLG) and sodium titanate (NaTi) coated titanium alloys, *in vitro.* ***Methods and materials:*** PDL cells were cultured with DMEM media containing 10% FBS on the S, SSG, SLG and NaTi titanium surfaces. PDL cell proliferation, mineralization and immunohistochemistry experiments for Bone Sialoprotein (BSP) were performed. The morphology of the PDL cells was examined using confocal and scanning electron microscopy (SEM). Gene expression profiles of cells were evaluated using a quantitative-polymerase chain reaction (Q-PCR) for type I collagen (COL I), Osteocalcin (OCN), osteopontin (OPN) and Runt-related transcription factor-2 (Runx2) on days 7 and 14. ***Results.*** Proliferation results on days 6 and 10 were similar in groups, while those of day 13 revealed a decrease in the NaTi group when compared to the S group. NaTi surface induced BSP mRNA expression which was correlated with mineralization tests and BSP immunostaining results. Increased Runx2 mRNA expression was also noted in the NaTi surface when compared to other surfaces. ***Conclusions.*** This study considers the NaTi surface as a potential alternative to SSG and SLG surfaces. This surface might provide a promising environment for PDL ligament-anchored implants.

Key Words: *titanium surface, sodium titanate coating, implant, periodontal ligament cells, scanning electron microscopy, confocal microscopy, proliferation, mineralization, mRNA expressions*

Introduction

Surface properties of titanium implants play an important role for their long-lasting attachment to peri-implantal tissues [1]. Surface topography of the implant may modify cell attachment, orientation, spreading, proliferation, differentiation and protein expressions related with mineralized tissues [2]. The range of micro-roughness maximizes the interlocking between mineralized bone and implant surfaces [3]. Today, micro-rough implant surfaces are generally used in the dental implant market [4,5]. Micrometer level surface topography results in greater growth of bone at the implant surface is supported by some clinical evidence [6]. A variety of methods have been developed in order to create surface roughness to improve the bone behavior of dental implants. The methods used to create a certain surface roughness for titanium dental implants are, for example, titanium plasma spraying, blasting with ceramic particles, acid etching and anodization [7]. The coating of the titanium implant surface has been reported to provide a microporous surface of increased bioactivity resulting in high rates of osteoconduction and big bonding

Correspondence: Professor Sema S. Hakki, DDS, PhD, Selcuk University, Faculty of Dentistry, Department of Periodontology, Konya, 42079, Turkey. E-mail: sshakki@yahoo.com; sshakki@selcuk.edu.tr

(Received 8 May 2012; revised 6 July 2012; accepted 21 August 2012)

ISSN 0001-6357 print/ISSN 1502-3850 online
DOI: 10.3109/00016357.2012.734417

forces at the interface between the implant and the newly formed bone tissue. In addition, the sodium titanate (NaTi) coating provides enhanced wetting and a surface with controlled roughness characteristics. Research demonstrated that NaOH-treated titanium exhibited a microporous network and the calcium phosphate deposits were greater for the NaOH-treated than for the commercially pure titanium [8–10].

Increase in roughness on the surface of titanium implants significantly improves cellular attachment and osseointegration [1,11,12]. The behavior of cellular population in contact with a metal depends directly on the microscopic properties of implants, such as topography, chemicals and surface energy [4,5]. While the effects of different types of surface treatments of titanium have been well-defined in osteoblastic cells and mesenchymal stem/stromal cells [13–20], studies focused on periodontal ligament (PDL) cells–titanium surface interactions are limited [21–24].

The periodontal ligament is a non-mineralized connective tissue that is present between two mineralized tissues; the alveolar bone and the cementum. Several studies [25–30] demonstrated that PDL cells have the capacity to differentiate to osteoblasts and/or cementoblasts. Characterization studies of PDL cells *in vitro* showed that these cells have osteoblast-like features including synthesis and expression of alkaline phosphatase (ALP) and osteopontin (OP), 1,25 dihydroxyvitamin D3 -induced bone Gla protein synthesis, responsiveness to parathyroid hormone (PTH) and dexamethasone (Dex)-induced PTH-mediated cAMP synthesis [31]. Moreover, PDL cells have the capacity to produce mineralized nodules *in vitro* [32,33].

A recently proposed approach in dental implantology is to bioengineer PDL tissues on titanium implants in order to improve current implant practice by mimicking the natural teeth [34–36]. The results of studies [35,36] performed on rats and dogs to create a periodontal ligament interface between the dental implant and bone demonstrated that cells derived from PDL tissue on titanium implants have a capacity to form cementum-like tissue, PDL tissue with Sharpey's fibers and new bone formation.

New implant surfaces undergo *in vitro* and *in vivo* evaluation in the literature to improve cell/surface harmony [37–42]. The purpose of this study was to investigate proliferation, morphology, mineralization and mRNA expression of mineralized tissue associated proteins mRNA expressions including type I collagen (COL I), bone sialoprotein (BSP), osteocalcin (OCN), osteopontin (OPN) molecules and runt-related transcription factor-2 (Runx2) of PDL cells on smooth (S), sandblasted small-grit (SSG; blasted with 100 μm alumina particles), sandblasted large-grit (SLG; blasted with 300 μm alumina particles) and NaTi coated titanium alloys *in vitro*.

Materials and methods

Cell isolation and culture

Human PDL cells were isolated from healthy periodontal ligaments of premolar extracted for orthodontic reasons [25,31–33]. Patients were informed of the study and a written consent was obtained. After extraction, the teeth were placed into biopsy media (Dulbecco's Modified Eagles Media [DMEM] (Biological Industries, Israel) with 10% fetal bovine serum [FBS] (Biological Industries), 250 μg/ml gentamicin sulfate, 5 μg/ml amphotericin B, 100 units/ml penicillin (Biological Industries), 100 μg/ml streptomycin (Biological Industries)). The periodontal ligament attached to the middle third of the root was removed with a scaler to avoid contamination with gingival and apical tissues. The PDL tissue was cut into small pieces, rinsed with biopsy media and placed into tissue culture dishes. PDL tissues were incubated in biopsy medium in a humidified chamber at an atmosphere of 95% air and 5% CO_2 at 37°C overnight. The following day, the biopsy medium was replaced with culture medium (DMEM with 10% FBS, 100 units/ml penicillin, 100 μg/ml streptomycin). After reaching confluency, cells were passaged with 0.25% trypsin and 0.1% ethylene diaminotetraacetic acid (EDTA). PDL cells of the 4th and the 7th passage were used in the experiments.

Preparation of the titanium discs

Commercially-available titanium alloy Ti6Al4V (ISO 5832-3, ASTM F67; Acnis International, Villeurbanne, France) was cut into 1 mm thick discs of 10 mm diameter. These discs were divided into four experimental groups as follows;

(1) Electro-polished smooth (S) surface group;
(2) Sandblasted small-grit (SSG), using 100 μm size alumina (Al_2O_3) particles;
(3) Sandblasted large-grit (SLG) using 300 μm size alumina (Al_2O_3) particles; and
(4) Sodium titanate coated (NaTi) group. For sodium titanate coating, the Ti6Al4V alloy discs were immersed in 5N NaOH solution for 48 h at 60°C and after drying in an oven at 105°C, treated thermally at 600°C for 2 h. The NaTi coating was crystalline and consisted predominantly of the $Na_2O.6TiO_2$ phase as ascertained from the XRD patterns. All discs were mechanically cleaned and gamma sterilized prior to tests [15].

Surface characterization

Implants were evaluated with a JSM-6400 electron microscope (JEOL) equipped with the NORAN 6 X-ray Microanalysis System and Semafore Digitizer (Figure 1). Surface properties were recorded and EDS

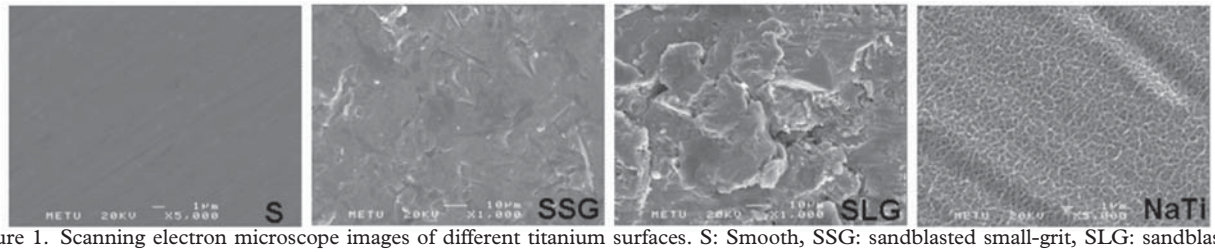

Figure 1. Scanning electron microscope images of different titanium surfaces. S: Smooth, SSG: sandblasted small-grit, SLG: sandblasted large-grit, NaTi: sodium titanate surfaces. This figure was modified from Korkusuz et al.'s [15] study.

analysis was conducted. The roughness of the surfaces was measured using the Surftest SJ-301 Portable Surface Roughness Tester (Mitutoyo America Corporation) (Table I). A Rigaku D/MAX2200/PC x-ray diffractometer was available for studying the crystalline nature of the NaTi coatings.

Proliferation and mineralization tests

Proliferation assay. Discs were placed into 24 well plates and cells at the density of 50,000 cells/well were transferred onto the titanium surfaces and cultured. PDL cells were allowed to adhere to the discs for 3 days. The cell culture medium was changed at every other day after cell adhesion. Three samples were investigated for each time point and the average number of cells was recorded. Cells were counted with the Neauber hemocytometer using the trypan blue dye on days 2, 6 10 and 13.

Mineralization experiments. Cells were plated at a density of 5×10^4 cells per well in 24-well plates in DMEM containing 10% FBS. After the attachment to the surfaces, the cells were nourished with DMEM containing 5% FBS+ Mineralization Media [ascorbic acid (AA, 50 μg/ml) and b-glycerophosphate (10 mM)]. Mineralization of extracellular matrix was determined on day 24 by von Kossa staining [43]. The mineralization experiments were repeated twice in triplicate for each surface.

Morphologic analyses

Confocal microscopy (CM). PDL cell behavior on the surfaces was assessed by CM at 5, 21 and 48 h and on day 20. Six slices for each group were prepared. The samples were placed into Petri dishes and covered completely by fluorescent-labeled PDL cell suspension. PDL cells were fluorescent labeled as described previously [15,44] and kept in a humidified chamber at 37°C and 5% CO_2. Cells were incubated for 2 h at 37°C with dialkylcarbocyanine probe DiL (Invitrogen 10 μg/ml in serum-free culture medium). They were than re-suspended in control medium and plated into the Petri dishes over the slices. Dialkylcarbocyanine probes are amphilic molecules containing a charge fluorophore that localizes the probe at membrane's surface and lipophilic aliphatic tails that insert into the membrane and thus anchor the probe to the membrane. The dye dominantly labels the cell membrane. Depending on the division rate, membranous organelles were labeled by time in addition to the cell membrane. At the end of the incubation time slices were washed a couple of times in 0.01 M PBS and fixed for 15 min in 2.5% gluteraldehyde (in PBS). Then, they were washed with PBS, transferred onto glass bottom flasks and examined under a confocal laser-scanning microscope (LSM Pascal, Zeiss, Germany) for fluorescent imaging. A 543 nm laser-line was used for excitation and a 560 nm barrier filter was used for collecting the emitted fluorescence. A stack of focal image sections were acquired and 3D projection images were constructed subsequently for measurements. The length and the width of the cells were measured and the mean values of length/width ratio were presented to evaluate the development of typical spindle shape of the PDL cells.

Immunohistochemical characterization of extracellular matrix synthesis: BSP labeling. Immunohistological procedure used in this study was described in detail previously [45]. In brief, on day 20 of culture, PDL cells incubated on different surfaces were fixed by immersion with 0.02% paraformaldehyde solution in PBS (pH 7.0) at room temperature for 20 min. Samples were washed 3-times with 0.01 M PBS (pH 7.04) for 5 min. The cells were permeabilized with 0.2% triton X dissolved in 0.01 M PBS at 4°C for 20 min afterwards. After washing in PBS for 5 min, primary antibody incubation was carried out at an optimal concentration rabbit anti-human and rat polyclonal BSP [Bone sialoprotein; IgG Abcam ABD cat#

Table I. Surface roughness parameters of smooth (S), sandblasted small-grit (SSG), sandblasted large-grit (SLG) and sodium titanate (NaTi) coated samples.

Surfaces	Average roughness R_a (μm) ± SD	Maximum roughness Depth R_y (μm) ± SD
S	0.06 ± 0.01	0.42 ± 0.03
SSG	0.30 ± 0.04	1.91 ± 0.14
SLG	1.50 ± 0.16	6.21 ± 0.35
NaTi	0.40 ± 0.04	4.23 ± 0.32

Table II. Synthetic oligonucleotide primers for RT-PCR. All sequences are from human and listed 5'–3'.

Primer	Forward	Reverse
COL I	TTTGTGGACCTCCGGCTC	AAGCAGAGCACTCGCCCT
BSP	GCCTGTGCTTTCTCAATG	TTCCTTCCTCTTCCTCCTC
OCN	CATGAGAGCCCTCACA	AGAGCGACACCCTAGAC
OPN	CCCACAGACCCTTCCAAGTA	ATTCAACTCCTCGCTTTCCA
Runx2	CTTCATTCGCCTCACAAAC	GTCACTGCGCTGAAGA
GAPDH	ACCACAGTCCATGCCATCAC	TCCACCACCCTGTTGCTGTA

ab-52128,1/100] in glass bottom culture dishes suitable for CM examination [Mattek USA cat# MTP24G, Ashland MA] overnight at 4°C. After washing with 0.01 M PBS at pH 7.4, cell-metal composites were incubated with fluorescent labeled goat anti rabbit Ig G (Alexa Fluor 488 and 543 Molecular Probes USA, cat# A11008, 1/100) or goat anti mouse Ig G (Alexa Fluor 488 and 543 Molecular Probes, cat# A11001, 1/100) for 30 min at room temperature. All antibodies were diluted in a background reducing buffer solution in 0.05 M Tris-HCl containing 0.1% tween (#S3022, Dako, USA). Negative control staining was performed by omitting the initial primary antibody staining step and using a control mouse Ig G. Positive control staining was performed by using cultured PDL cells only.

Accordingly each sample was graded for cellular immune reaction on a scale of 0 to +++ with Alexa fluor [45]. 0 was given to no immune reactivity, + to weak but continuous reactivity, ++ for moderate but continuous reactivity and +++ to intense but continuous immunostaining. The number of immune positive cells was expressed as a percentage of positive cells over total cells at 200 × magnification. In every specimen the average of three non over-lapping fields was analyzed and reported.

Scanning electron microscopy (SEM). In order to assess the PDL cell attachment and behavior on different surfaces at the ultrastructural level, the discs were fixed for 15 min with 2.5% glutaraldehyde. After removal from the petri dishes, the samples were dried and sputter-coated with gold. The SEM study was conducted with a JSM-6400 Electron Microscope (JEOL), equipped with the NORAN 6 X-ray Microanalysis System and Semafore Digitizer. The PDL cell-discs surface interaction was examined at 6, 24 and 48 h and on day 20.

Gene analyses

RNA Isolation. For each surface group, three titanium discs were placed in 60 mm cell culture dishes and PDL cells were plated at 2.5×10^4 cells/cm^2 and incubated for 3 days without moving. Total RNAs from different titanium surface groups were isolated at passage 4–7 on days 7 and 14, using a monophasic solution of phenol and guanidine isothiocyanate (Invitrogen, CA, USA) [26]. Total RNA was quantified at 260 nm by spectrophotometer. RNA samples were stored at −70°C.

cDNA synthesis and quantitative RT- PCR analysis. For real time RT-PCR analysis, cDNA was synthesized from 1.0 μg of total RNA with a cDNA synthesis kit (High Capacity RNA-to-cDNA kit; Applied Biosystems, Foster City) for RT-PCR. From the resulting cDNA product, 1.0 μl was used per 25 μl final reaction volume in the thermal cycler (Stratagene, TX). PCR reactions were carried out with the Brilliant SYBR Green QPCR Master Mix kit (Stratagene), in a total volume of 25 μl. Primers were designed using DNA-Star software and sequences are listed in Table II. A BLAST search of GenBank was performed on the primer sequences to ensure specificity. Glyceraldehyde-3-phosphate dehydrogenase (GAPDH) served as a housekeeping/reference gene for normalization. Amplification profiles for PCR were optimized for primer sets. Amplification was completed with a final extension step of 8 min at 72°C. The amplification profile for Osteocalcin (OCN), Runt-related transcription factor 2 (RunX2), collagen type I (COL I) and GAPDH used on the Stratagene MX3000P was 94°C for 3 min followed by 35 cycles of 94°C/45 s, 54°C/45 s and 72°C/1 min. Amplification was completed with a final extention step of 10 min at 72°C. The amplification profile for Bone Sialoprotein (BSP), Osteopontin (OPN) and GAPDH used on the Stratagene MX3000P was 94°C for 3 min followed by 40 cycles of 94°C/45 s, 52°C/45 s and 72°C/1 min. Amplification was completed with a final extention step of 10 min at 72°C. Quantitative RT-PCR experiments were repeated twice.

Statistical analysis

One-way analysis of variance (ANOVA) and Tukey HSD multiple comparison tests were used to compare groups.

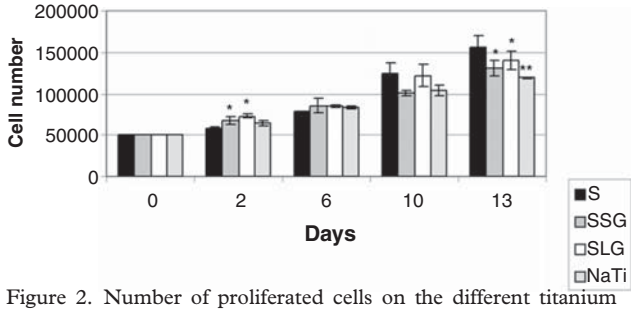

Figure 2. Number of proliferated cells on the different titanium surfaces on days 2, 6, 10 and 13. The data are represented as mean ± standard deviation. * Represents a statistically significant difference ($p < 0.05$) compared with the S surface. ** Represents a statistically significant difference ($p < 0.01$) compared with the S surface.

Results

Proliferation and mineralization analyses

On day 2, a significant increase in cell proliferation of PDL cells was noted in SSG and SLG surfaces when compared to the S surface. Proliferation experiments did not reveal any statistical difference between groups on days 6 and 10. On day 13, a decreased proliferation rate was observed in the SSG, SLG ($p < 0.05$) and NaTi group when compared to the S group (Figure 2). This decrease was more evident in the NaTi surface ($p < 0.01$).

However quantitative evaluation was not performed and von Kossa staining macroscopically revealed slight increase in mineralized nodules on the NaTi group when compared to the other groups (Figure 3).

Morphologic analyses

Confocal microscopy analysis. The DiL labeled PDL cells scattered as different sized clusters on titanium surfaces from the 5th hour. Length/width ratios of SSG and SLG surfaces were higher when compared to S and NaTi surfaces at 5 h. At 21 h, while a higher ratio was observed in the S surface, a decreased ratio was observed in the SSG and SLG surfaces ($p < 0.05$) and a more pronounced reduction in length/width ratio was noted in the NaTi surface ($p < 0.01$). The shape of the PDL cells was more cuboidal on the NaTi surface. At 48 h, there was no apparent difference among the groups (Figures 4A and B). The attached cell population, interconnected with their cytoplasmic processes, increased in time and formed a multilayer with a high amount of extracellular matrix on the discs on day 20 (Figure 4C). The PDL cells formed a stronger network on the NaTi surface compared to the other groups on day 20 (Figure 4C). Both the SSG and the NaTi groups surfaces were covered by a thicker multilayered connective tissue compared to that of the S group (Figure 4C).

Immunohistochemistry: BSP labeling. The BSP, which is a marker for a potentially mineralizing matrix, exhibited a wide and moderate-to-strong cytoplasmic expression pattern in the PDL cells attached to the titanium surfaces on day 20. The PDL cells cultured on the sand-blasted (SSG and SLG) and the NaTi surfaces exhibited higher BSP immunoreactivity when compared to that of the polished surface (Figure 5, Table III).

SEM analysis. The spindle-shaped PDL cells attached to the titanium discs at ~ 6 h after seeding. The PDL cells anastomosed with each other by their cytoplasmic extensions and migrated into the grooves of the smooth sand-blasted, rough sand-blasted and sodium titanate coated surfaces of the discs at 24 and 48 h (Figure 6A). The interconnected cells composed multiple layers by secreting their extracelluar matrix on the surfaces on day 20 (Figure 6B). The attached cell population lying with their cytoplasmic extensions was more intense on the polished surface at the 6th hour than that of the sodium titanate modified surface displaying cell groups with more round morphology (Figure 6A). The cellular cytoplasmic extensions and extracellular matrix production was higher than that of the polished surface on the sand-blasted surfaces with no significant difference in between the smooth and rough sand-blasted groups. On day 20, Na titanate coated surface provided the best environment for PDL cell alignment and extracellular matrix production exhibiting the thicker cellular layer when compared to that of the control and sandblasted groups.

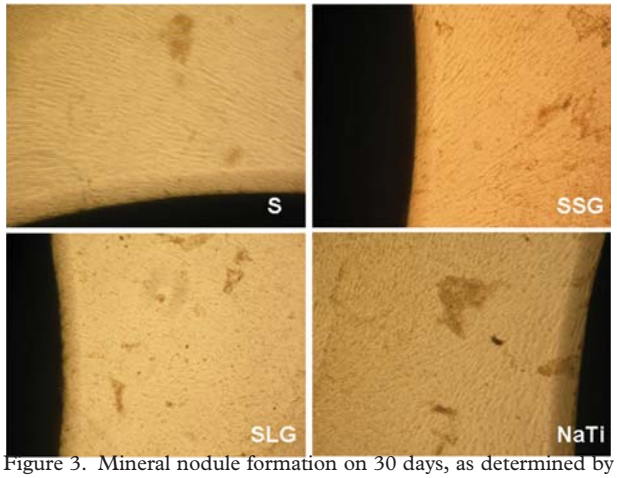

Figure 3. Mineral nodule formation on 30 days, as determined by von Kossa staining. DMEM containing 5%FBS, β-glycerophoshate (β-GP, 10 mM) and ascorbic acid (AA, 50 μg/ml) was used as mineralization media. More mineral-like nodules were observed in NaTi surfaces.

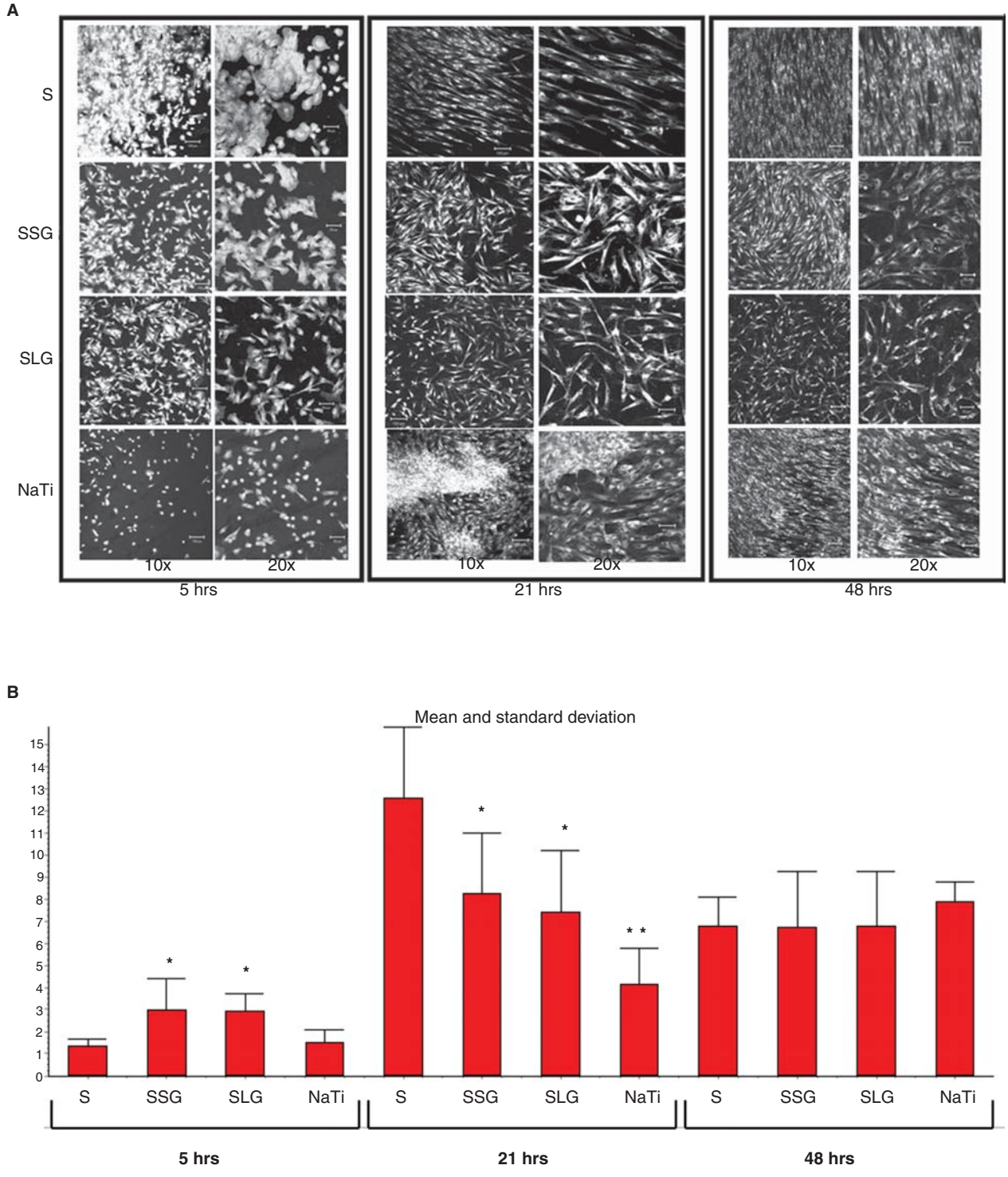

Figure 4. (A) Confocal microscope images of PDL cells on the different titanium surfaces at 5, 21 and 48 h with 10 × and 20 × magnifications. (B) Length/width ratio of PDL cells on the root slices (bar: mean ± SD). At 5 h, the ratios of S and NaTi surfaces were similar and lower than that of SSG and SLG surfaces which were also similar. At 21 h, a higher ratio was observed in the S surface, a decreased ratio was observed in the SSG and SLG surfaces ($p < 0.05$) and a more pronounced reduction in length/width ratio was noted in the NaTi surface ($p < 0.01$). The shape of the PDL cells was more cuboidal on the NaTi surface. At 48 h, no obvious difference was noted among the titanium surfaces. * Represents a statistically significant difference ($p < 0.05$), ** represents a statistically significant difference ($p < 0.01$). (C) DiL staining of PDL cells on day 20.

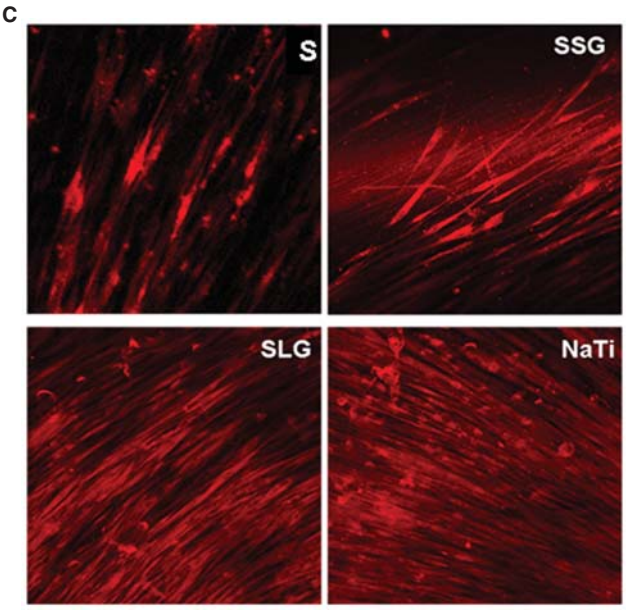

Figure 4. (*Continued*).

mRNA expressions on days 7 and 14 (Figure 7)

- *Bone sialoprotein* (BSP): There was a tendency to increase in rough surfaces when compared to the S surface and this increase was more evident in NaTi surfaces ($p < 0.05$), especially on day 7. BSP mRNA expressions in both SSG and SLG surfaces look similar. On day 14 there was no significant difference among the groups;
- *Type I collagen* (COL I): While COL I mRNA expression decreased in SSG surfaces in both time points, there was no significant difference between the surfaces;
- *Osteoblastic transcription factor* (Runx2): Increased Runx2 mRNA expression was observed in the NaTi group when compared to S, SSG and SLG surfaces on days 7 and 14. This increase was statistically significant ($p < 0.001$) on day 14;
- *Osteocalcin* (OCN): OCN mRNA expressions look similar in the groups when compared to control and S surfaces. Only on day 14 was a significant decrease in OCN mRNA expression observed in the NaTi group.
- *Osteopontin* (OPN): While there was a statistically significant increase in SSG and SLG surfaces ($p < 0.001$), when compared to the S surface, decreased OPN transcripts in the NaTi group was observed. The expression levels of the NaTi surface were similar to the S group.

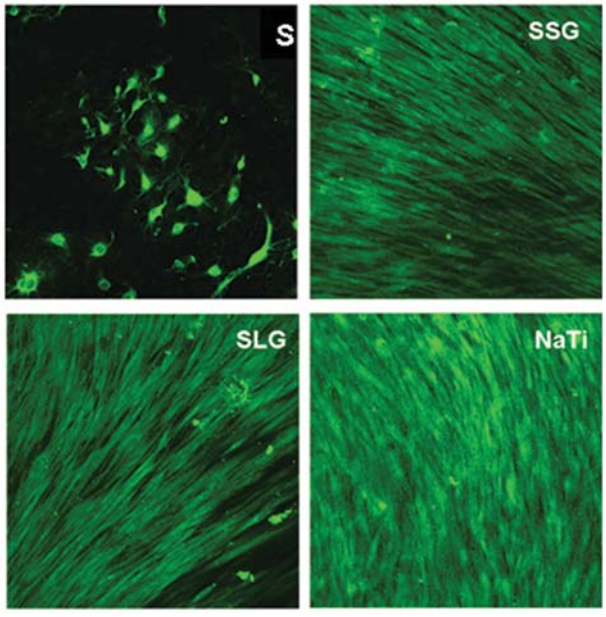

Figure 5. BSP immune-staining on day 20. Note the increased BSP staining in SSG, SLG and NaTi surfaces. A more evident increase was examined in NaTi surfaces. This BSP staining confirmed mRNA expressions of BSP using QPCR on days 7 and 14.

Discussion

Nowadays, osseointegration is considered as a critical biological process for implant success and stability; however, to attach PDL cells and subsequently to form organized PDL tissue on titanium implants would be superior to current implant therapies. Therefore, the idea was whether PDL cells can be used to constitute PDL tissues on titanium implants to mimic naturally-formed teeth [34–36]. If this idea can be an alternative approach to osseointegrated implants, to learn an optimal surface for PDL cells is critical to develop novel clinical methods.

Different surface modifications including SSG, SLG and NaTi were evaluated in this study for PDL cells and we found that PDL cells were biocompatible with all surfaces and a slight increase was noted in mineralized nodules in the NaTi group when compared to other groups. In our previous study, we investigated the interaction of the same surfaces with MC3T3-E1 cells [15] and we observed that sand-blasting and sodium titanate coating provided by NaOH favors the attachment, mineralization and early differentiation of osteoblasts on titanium alloys. Moreover, based on the results of our studies, we claim that PDL cells have also osteoblast-like characteristics regarding the response to different titanium surfaces.

Surface roughness not only influences cell attachment, adhesion, proliferation, differentiation and matrix synthesis, but also affects cell orientation and migration [46]. The exact role of surface

Table III. The immunohistological scores related to BSP labeling are presented.

	Polished	SSG	SLG	NaTi
BSP labeling	++	++/+++	++/+++	+++

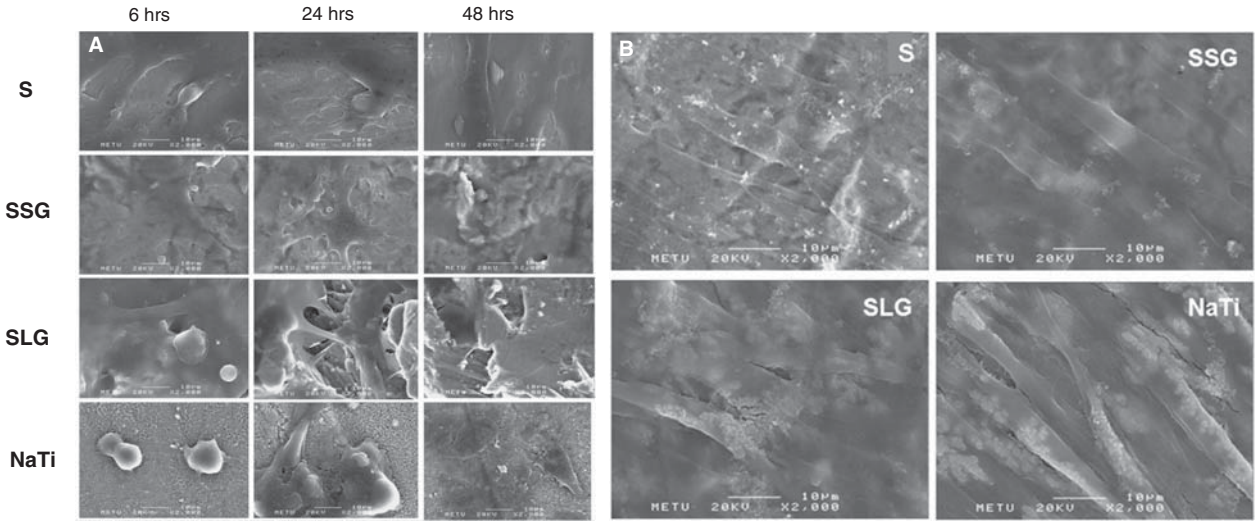

Figure 6. (A) Scanning electron microscope images of PDL cells on the different titanium surfaces at 6, 24 and 48 h with × 2000 (Scale bar = 10 μm). (B) Scanning electron microscope images of PDL cells on the different titanium surfaces on day 20 with × 2000 (Scale bar = 10 μm).

roughness, however, is controversial since some studies reported that smoother surfaces increase cell proliferation, while others concluded with opposite results. Osteoblasts did not spread completely on rough surfaces and acquired a polygonal morphology with diminished cell proliferation rate [16,17,47]. Hence, the cells may differentiate and synthesize a more mineralized matrix on rough surfaces when compared

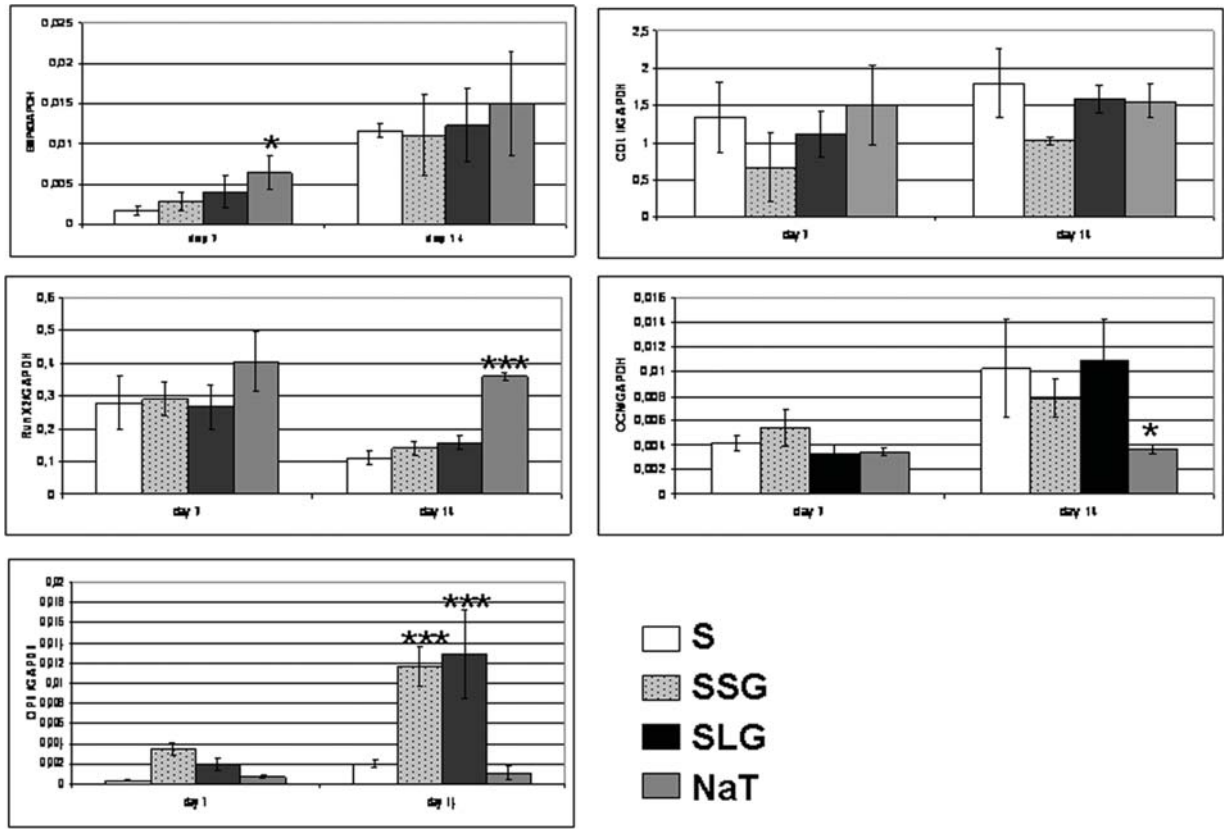

Figure 7. Mineralized tissue-associated proteins mRNA expressions (bone sialoprotein [BSP], type I collagen [COLI], osteocalcin [OCN], osteopontin [OPN]) and osteoblastic transcription factor (Runx2) of PDL cells using Q-PCR on days 7 and 14. Each bar represents the mean ± standard deviation. * Represents a statistically significant difference ($p < 0.05$) compared with the S surface. *** Represents a statistically significant difference ($p < 0.001$) compared with the S surface.

to smooth surfaces. In contrast, Deligianni et al. [48] reported that more bone marrow cells adhered on to the rough titanium surface than on the smoother one. Decreased proliferation rates were observed in the SSG, the SLG and the NaTi groups on days 10 and 13 when compared to the S group ($p < 0.05$), while on days 2 and 6 there were no apparent differences among the groups in our study. This reduction in cell proliferation was more pronounced in the NaTi group when compared to the S ($p < 0.01$), SSG and SLG groups. Variances in the results of the studies may be observed due to the cell type utilized, the origin of the cells and the time points examined.

Type I collagen, bone sialoprotein and ostepontin play important roles during osteogenesis and osseointegration processes [49]. The expression of BSP is highly specific for mineralized tissues. Highest BSP expression is found in the newly synthesized and regenerated bone matrix. Regarding BSP mRNA expressions, there was a tendency of increase in NaTi surfaces, especially on day 7. BSP mRNA expressions in both SSG and SLG surfaces were similar. Only on day 14 was a significant decrease in OCN mRNA expression observed in the NaTi group. While there was a statistically significant increase in SSG and SLG surfaces when compared to S surfaces, decreased OPN transcripts in the NaTi group was observed. The expression levels of the NaTi surface were similar to the S group. Increased Runx2 mRNA expressions were observed in the NaTi group when compared to other surfaces on day 7. A strong increase ($p < 0.001$) in Runx2 mRNA expression on day 14 was noted. Correlating proliferation and mineralization results with mRNA expression for mineralized tissue-associated markers, NaTi surface induced BSP mRNA expression and protein level when compared to other surfaces.

Isa et al. [50] investigated human embryonic palatal mesenchymal cells on the surfaces including grit-blasted with titanium dioxide (TiO_2-blasted) and fluoride-modified titanium surfaces for cell proliferation, alkaline phosphatase (ALP)-specific activity and mRNA steady-state expression for bone-related genes (ALP, type I collagen, osteocalcin, bone sialoprotein [BSP] II, Cbfa1 and osterix) by Q-PCR. Their results demonstrated that, while the different surfaces did not alter the mRNA expression for ALP, type I collagen, osterix, osteocalcin or BSP II, Cbfa1 (a key regulator for osteogenesis, Runx2), expression on the fluoride-modified titanium surface was significantly higher ($p < 0.001$) at 1 week. The number of cells on this surface was 20% lower than the number of cells on the surface TiO2-blasted. In our study, BSP transcript at 1 week and Runx2 transcript at 2 weeks were significantly higher in the NaTi surface when compared to other surfaces. Furthermore, the number of cells on the NaTi surface was significantly lower when compared to the other groups.

In another newly-established titanium surface study undertaken by Park et al. [37], titanium surfaces incorporated with strontium ions (Sr) and/or phosphate ions (P) produced by hydrothermal treatment were evaluated. These researchers investigated MC3T3-E1 pre-osteoblast cell attachment, morphology of spread cells, viability and quantitative analysis of osteoblastic gene expression on grit-blasted micro-rough (RBM), P-incorporated (P) and P- and Sr-incorporated (SrP) Ti surfaces. Sr incorporation significantly increased cellular attachment and viability compared with other surfaces ($p < 0.05$). Q-PCR results demonstrated markedly higher mRNA expressions of the osteoblast transcription factor gene (Runx2) and the osteoblast phenotype genes (alkaline phosphatase, osteopontin, bone sialoprotein and osteocalcin) in cells grown on the P and SrP surfaces compared with those on the RBM surface. However, we evaluated different titanium surfaces in our study, we observed reduced cell proliferation in the NaTi surface and increased BSP and Runx2 (Cbfa1) mRNA expressions in this surface when compared to sand-blasted and smooth surfaces.

Since the PDL ligament-anchored implants might mimic the natural insertion of tooth roots in alveolar bone [34,51,52], we believe that the investigation of PDL cell behavior and interaction between different titanium implant surfaces provided valuable information. In the present study, we observed increased BSP and Runx2 mRNA expressions related with increased bio-mineralization in the NaTi group. Our results demonstrated that NaTi surface might provide a promising environment for PDL ligament-anchored implants in the future by regulating the proliferation rate, morphology and differentiation of PDL cells. Cell culture studies are valuable to investigate the biological interaction of new titanium surfaces/cells and provide to gain an initial insight regarding cell morphology, adhesion, migration, proliferation and differentiation on implant surfaces [7,53]. However, cell culture studies can not simulate the dynamic environment of bone/implant surface and *in vivo* performance of modified/novel implant surfaces should be confirmed in animal models and subsequent clinical trials.

Acknowledgement

This study was performed at the Research Laboratory of Faculty of Dentistry, Selcuk University and was supported by Turkish Scientific Research Council (TUBITAK-SBAG/3130).

***Declaration of interest*:** The authors report no conflicts of interest. The authors alone are responsible for the content and writing of the paper.

References

[1] Zhao JM, Tsuru K, Hayakawa S, Osaka A. Modification of Ti implant surface for cell proliferation and cell alignment. J Biomed Mater Res A 2008;84:988–93.

[2] Oates TW, Maller SC, West J, Steffensen B. Human gingival fibroblast integrin subunit expression on titanium implant surfaces. J Periodontol 2005;76:1743–50.

[3] Wennerberg A, Hallgren C, Johansson C, Danelli S. A histomorphometric evaluation of screw-shaped implants each prepared with two surface roughnesses. Clin Oral Implants Res 1998;9:11–19.

[4] Albrektsson T, Wennerberg A. Oral implant surfaces: part 1–review focusing on topographic and chemical properties of different surfaces and *in vivo* responses to them. Int J Prosthodont 2004;7:536–43.

[5] Albrektsson T, Wennerberg A. Oral implant surfaces: part 2–review focusing on clinical knowledge of different surfaces. Int J Prosthodont 2004;17:544–64.

[6] Wennerberg A, Albrektsson T. On implant surfaces: a review of current knowledge and opinions. Int J Oral Maxillofac Implants 2010;25:63–74.

[7] Junker R, Dimakis A, Thoneick M, Jansen JA. Effects of implant surface coatings and composition on bone integration: a systematic review. Clin Oral Implants Res 2009;20: 185–206.

[8] Dadgostrai S. MS Thesis, Graduate Department of Dentistry, Institute of Biomaterials and Biomedical Engineering. Toronto: University of Toronto; 2000.

[9] de Andrade MC, Filgueiras MR, Ogasawara T. Nucleation and growth of hydroxyapatite on titanium pretreated in NaOH solution: experiments and thermodynamic explanation. J Biomed Mater Res 1999;46:441–6.

[10] Ho WF, Lai CH, Hsu HC, Wu SC. Surface modification of a Ti-7.5Mo alloy using NaOH treatment and Bioglass coating. J Mater Sci Mater Med 2010;21:1479–88.

[11] Brunski JB. *In vivo* bone response to biomechanical loading at the bone/dental-implant interface. Adv Dent Res 1999;13:99–119.

[12] Cochran DL, Buser D, ten Bruggenkate CM, et al. The use of reduced healing times on ITI implants with a sandblasted and acid-etched SLA] surface: early results from clinical trials on ITI SLA implants. Clin Oral Implants Res 2002;13:144–53.

[13] Maekawa K, Yoshida Y, Mine A, van Meerbeek B, Suzuki K, Kuboki T. Effect of polyphosphoric acid pre-treatment of titanium on attachment, proliferation, and differentiation of osteoblast-like cells MC3T3-E1]. Clin Oral Implants Res 2008;19:320–5.

[14] Galli C, Guizzardi S, Passeri G, et al. Comparison of human mandibular osteoblasts grown on two commercially available titanium implant surfaces. J Periodontol 2005;76:364–72.

[15] Korkusuz P, Hakki SS, Purali N, et al. Interaction of MC3T3-E1 cells with titanium implants. Joint Dis Related Surg 2008;19:84–90.

[16] Anselme K, Linez P, Bigerelle M, et al. The relative influence of the topography and chemistry of TiAl6 V4 surfaces on osteoblastic cell behaviour. Biomaterials 2000;21:1567–77.

[17] Bächle M, Kohal RJ. A systematic review of the influence of different titanium surfaces on proliferation, differentiation and protein synthesis of osteoblast-like MG63 cells. Clin Oral Implants Res 2004;15:683–92.

[18] Balloni S, Calvi EM, Damiani F, et al. Effects of titanium surface roughness on mesenchymal stem cell commitment and differentiation signaling. Int J Oral Maxillofac Implants 2009;24:627–35.

[19] Giannoni P, Muraglia A, Giordano C, et al. Osteogenic differentiation of human mesenchymal stromal cells on surface-modified titanium alloys for orthopedic and dental implants. Int J Artif Organs 2009;32:811–20.

[20] Guizzardi S, Galli C, Martini D, et al. Different titanium surface treatment influences human mandibular osteoblast response. J Periodontol 2004;75:273–82.

[21] Michaels CM, Keller JC, Stanford CM. *In vitro* periodontal ligament fibroblast attachment to plasma-cleaned titanium surfaces. J Oral Implantol 1991;17:132–9.

[22] Hoshi N, Negishi H, Okada S, Nonami T, Kimoto K. Response of human fibroblasts to implant surface coated with titanium dioxide photocatalytic films. J Prosthodont Res 2010;54:185–91.

[23] Kramer PR, Janikkeith A, Cai Z, Ma S, Watanabe I. Integrin mediated attachment of periodontal ligament to titanium surfaces. Dent Mater 2009;25:877–83.

[24] Docheva D, Padula D, Popov C, et al. Establishment of immortalized periodontal ligament progenitor cell line and its behavioural analysis on smooth and rough titanium surface. Eur Cell Mater 2010;19:228–41.

[25] Hakki SS, Hakki EE, Nohutcu RM. Regulation of matrix metalloproteinases and tissue inhibitors of matrix metalloproteinases by basic fibroblast growth factor and dexamethasone in periodontal ligament cells. J Periodontal Res 2009;44:794–802.

[26] Lang H, Schuler N, Arnhold S, Nolden R, Mertens T. Formation of differentiated *tissues in vivo* by periodontal cell populations cultured *in vitro*. J Dent Res 1995;74:1219–25.

[27] Lin WL, McCulloch CA, Cho MI. Differentiation of periodontal ligament fibroblasts into osteoblasts during socket healing after tooth extraction in the rat. Anat Rec 1994; 240:492–506.

[28] Mariotti A, Cochran DL. Characterization of fibroblasts derived from human periodontal ligament and gingiva. J Periodontol 1990;61:103–11.

[29] Melcher AH. Repair of wounds in the periodontium of the rat. Influence of periodontal ligament on osteogenesis. Arch Oral Biol 1970;15:1183–204.

[30] Nojima N, Kobayashi M, Shionome M, Takahashi N, Suda T, Hasegawa K. Fibroblastic cells derived from bovine periodontal ligaments have the phenotypes of osteoblasts. J Periodontal Res 1990;25:179–85.

[31] Nohutcu RM, Somerman MJ, McCauley LK. Dexamethasone enhances the effects of parathyroid hormone on human periodontal ligament cells *in vitro*. Calcif Tissue Int 1995;56: 571–7.

[32] Nohutcu RM, McCauley LK, Shigeyama Y, Somerman MJ. Expression of mineral-associated proteins by periodontal ligament cells: *in vitro* vs. *ex vivo*. J Periodontal Res 1996;31: 369–72.

[33] Nohutcu RM, McCauley LK, Koh AJ, Somerman MJ. Expression of extracellular matrix proteins in human periodontal ligament cells during mineralization *in vitro*. J Periodontol 1997;68:320–7.

[34] Giannobile WV. Getting to the root of dental implant tissue engineering. J Clin Periodontol 2010;37:747–9.

[35] Gault P, Black A, Romette JL, et al. Tissue-engineered ligament: implant constructs for tooth replacement. J Clin Periodontol 2010;37:750–8.

[36] Lin Y, Gallucci GO, Buser D, Bosshardt D, Belser UC, Yelick PC. Bioengineered periodontal tissue formed on titanium dental implants. J Dent Res 2011;90:251–6.

[37] Park JW, Kim YJ, Jang JH. Enhanced osteoblast response to hydrophilic strontium and/or phosphate ions-incorporated titanium oxide surfaces. Clin Oral Implants Res 2010;21: 398–408.

[38] Park JW, Kim YJ, Jang JH, Kwon TG, Bae YC, Suh JY. Effects of phosphoric acid treatment of titanium surfaces on surface properties, osteoblast response and removal of torque forces. Acta Biomater 2010;6:1661–70.

[39] Park JW, Kim YJ, Jang JH, Suh JY. Surface characteristics and primary bone marrow stromal cell response of a nanostructured strontium-containing oxide layer produced on a

microrough titanium surface. J Biomed Mater Res A 2012; 100:1477–87.
[40] Mendonça G, Mendonça DB, Aragão FJ, Cooper LF. The combination of micron and nanotopography by H[2]SO[4]/H[2]O[2] treatment and its effects on osteoblast-specific gene expression of hMSCs. J Biomed Mater Res A 2010;94:169–79.
[41] Olivares-Navarrete R, Hyzy S, Wieland M, Boyan BD, Schwartz Z. The roles of Wnt signaling modulators Dickkopf-1 [Dkk1] and Dickkopf-2 [Dkk2] and cell maturation state in osteogenesis on microstructured titanium surfaces. Biomaterials 2010;31:2015–24.
[42] Taxt-Lamolle SF, Rubert M, Haugen HJ, Lyngstadaas SP, Ellingsen JE, Monjo M. Controlled electro-implementation of fluoride in titanium implant surfaces enhances cortical bone formation and mineralization. Acta Biomater 2010;6:1025–32.
[43] Hakki SS, Berry JE, Somerman MJ. The effect of enamel matrix protein derivative on follicle cells in vitro. J Periodontol 2001;72:679–87.
[44] Hakki SS, Korkusuz P, Berk G, et al. Comparison of Er,Cr: YSGG laser and hand instrumentation on the attachment of periodontal ligament fibroblasts to periodontally diseased root surfaces: an *in vitro* study. J Periodontol 2010;81:1216–25.
[45] Tokgözoğlu L, Can I, Korkusuz P, Aşan E, Ozer N, Demircin M. Correlation of tissue selectin expression and hemodynamic parameters in rheumatic mitral valve disease. J Heart Valve Dis 2006;15:1–7.
[46] Takamori ER, Cruz R, Gonçalvez F, Zanetti RV, Zanetti A, Granjeiro JM. Effect of roughness of zirconia and titanium on fibroblast adhesion. Artif Organs 2008;32:305–9.
[47] Sader MS, Balduino A, Soares G de A, Borojevic R. Effect of three distinct treatments of titanium surface on osteoblast attachment, proliferation, and differentiation. Clin Oral Implants Res 2005;16:667–75.
[48] Deligianni DD, Katsala N, Ladas S, Sotiropoulou D, Amedee J, Missirlis YF. Effect of surface roughness of the titanium alloy Ti-6Al-4V on human bone marrow cell response and on protein adsorption. Biomaterials 2001;22: 1241–51.
[49] Zhang T, Xia H, Wang Y, Peng C, Li Y, Pan X. Gene expression of four adhesive proteins in the early healing of bone defect and bone-implant interface. Conf Proc IEEE Eng Med Biol Soc 2006;1:2087–90.
[50] Isa ZM, Schneider GB, Zaharias R, Seabold D, Stanford CM. Effects of fluoride- modified titanium surfaces on osteoblast proliferation and gene expression. Int J Oral Maxillofac Implants 2006;21:203–11.
[51] Choi BH. Periodontal ligament formation around titanium implants using cultured periodontal ligament cells: a pilot study. Int J Oral Maxillofac Implants 2000;15: 193–6.
[52] Kim SH, Kim KH, Seo BM, Koo KT, Kim TI, Seol YJ, et al. Alveolar bone regeneration by transplantation of periodontal ligament stem cells and bone marrow stem cells in a canine peri-implant defect model: a pilot study. J Periodontol 2009; 80:1815–23.
[53] Palaiologou A, Stoute D, Fan Y, Lallier TE. Altered cell motility and attachment with titanium surface modifications. J Periodontol 2012;83:90–100.